

Dynamical magnetic relaxation: A nonlinear magnetically driven dynamo

Eric G. Blackman¹ and George B. Field²

1. Department of Physics & Astronomy and Laboratory for Laser Energetics, University of Rochester, Rochester NY 14627
2. Harvard-Smithsonian Center for Astrophysics, 60 Garden St. Cambridge MA, 02138

(in press, Physics of Plasmas)

ABSTRACT

A non-linear, time-dependent, magnetically driven dynamo theory which shows how magnetically dominated configurations can relax to become helical on the largest scale available is presented. Coupled time-dependent differential equations for large scale magnetic helicity, small scale magnetic helicity, velocity, and the electromotive force are solved. The magnetic helicity on small scales relaxes to drive significant large scale helical field growth on dynamical (Alfvén crossing) time scales, independent of the magnitude of finite microphysical transport coefficients, after which the growing kinetic helicity slows the growth to a viscously limited pace. This magnetically driven dynamo complements the nonlinear kinetic helicity driven dynamo; for the latter, the growing magnetic helicity fluctuations suppress, rather than drive, large scale magnetic helicity growth. A unified set of equations accommodates both types of dynamos.

PACS codes: 52.30.Cv, 95.30.Qd, 52.65Kj, 52.55 -s, 96.60.Hv, 98.62Mw

I. Introduction

The concept of dynamo means different things to different communities: In the astrophysical context, dynamo typically refers to the amplification of initially weak magnetic fields in a turbulent flow, but comes in two basic varieties: (1) small scale nonhelical (direct) dynamos in which magnetic energy is amplified by random walk field line stretching on spatial or temporal scales less than or equal to that of the turbulent forcing [1-4], and (2) large scale helical (inverse) dynamos [5-12], in which helical turbulence produces magnetic energy on scales larger than that of the input turbulent forcing. The latter is the type of dynamo needed to explain the large scale field and solar cycle of the sun. It thrives on a non-dissipative term in Ohm's law called the turbulent electromotive force (EMF), $\overline{\mathcal{E}}$, which equals the correlated average (time, space or ensemble) of the cross product of fluctuating velocity \mathbf{v} and fluctuating magnetic field \mathbf{b} , and is sustained by helical turbulence.

In fusion devices, the plasma is already magnetically dominated. Here the dynamo acts to convert magnetic flux from toroidal to poloidal (or vice versa), increase the scale of the field, and sustain the strong magnetic flux against microphysical dissipation [13-21]. Like the velocity-driven astrophysical helical dynamo, the magnetically dominated dynamo thrives on having a finite $\overline{\mathcal{E}}$ term in Ohm’s law, again resulting from correlated turbulent fluctuations possessing helicity (more on this later). But here the fluctuations are driven by current instabilities and magnetic helicity injection rather than kinetic helicity.

Although traditional astrophysical dynamos are normally studied for systems with initially weak magnetic fields, there are also important magnetically dominated astrophysical environments: astrophysical coronae. These include solar and stellar coronae, as well as coronae above accretion disks [23-25]. In coronae, the dynamo can convert and sustain flux, playing a similar role to the magnetically dominated dynamo in fusion devices. Coronal systems are magnetically driven in the sense that helical magnetic fields are injected from the disk or star below, and the subsequent time evolution is of interest. A key question is: how does the field open up and relax to large scales? This is relevant for the formation of magnetically driven jets and outflows from disks and stars.

It is useful to recognize that a magnetically dominated dynamo can also be thought of as dynamical magnetic relaxation. Magnetic relaxation describes the process by which magnetic structures in magnetically dominated environments evolve to their equilibrium states. The fully relaxed end state is the Taylor state [22], determined by minimizing the magnetic energy subject to the constraint that magnetic helicity is conserved. The result is a force-free helical configuration with the scale of the field reaching the largest scale available, subject to boundary conditions. But Taylor’s theory by itself is not a dynamical theory since it does not provide a time-dependent description of how the large scale magnetic helicity evolves. For that, a fully time dependent dynamo theory is needed. That is our goal herein.

In Ref. [12], a set of nonlinear dynamo equations for the growth of the large scale magnetic field was derived and solved when helical turbulent velocity forcing is applied. The nonlinear backreaction due to the build up of small scale magnetic helicity was shown to ultimately quench the large scale field growth, in quantitative agreement with numerical simulations [10, 11]. In the present paper, we study the complementary problem of large scale field growth from a dynamo driven by small scale magnetic helicity fluctuations. As we will show, the complementarity arises because the kinetic helicity becomes the quenching agent rather than the driving agent for the magnetic helicity driven dynamo. A novel feature of the present approach is that we include a fully time-dependent dynamical equation for the turbulent EMF which couples magnetic helicity and kinetic helicity, dynamically into the time dependent theory. Previous work on magnetically dominated dynamos focused on more specific magnetized configurations [13-21] in the steady-state in which $\overline{\mathcal{E}}$ is not solved for dynamically. We find that coupling the time evolution of $\overline{\mathcal{E}}$ into the theory is essential for understanding time-dependent magnetic relaxation.

We solve the dynamical nonlinear dynamo equations for a closed or periodic system. This

allows us to ignore boundary terms and will facilitate future testing of the basic principles with tractable 3-D numerical simulations. The theory is subtle enough, with enough new features, that we wish to present it for as simple a system as possible without focusing on detailed magnetic configurations and boundary terms. These will have to be considered in future work.

In section II we derive the coupled equations to be solved: the time evolution of large and small scale magnetic helicities, the turbulent EMF, and the kinetic helicity. In section III we discuss the solutions and the physical interpretation, and conclude in section IV.

II. Derivation of the Coupled Dynamical Equations to be Solved

We will use a simple multi-scale approach that has been relatively successful [12] in accounting for the non-linear dynamics of recent 3-D MHD helical dynamo simulations [10, 11] (and has been further shown to be reasonably consistent even compared to a theory in which 2 additional scales are included in the dynamics [26]): We write all quantities as the sum of large scale (indicated by overbar) and fluctuating (indicated by lower case) contributions. The vector potential \mathbf{A} , magnetic field $\mathbf{B} = \nabla \times \mathbf{A}$ (written in Alfvén units) and normalized current density $\mathbf{J} = \nabla \times \mathbf{B}$ then satisfy $\mathbf{A} = \overline{\mathbf{A}} + \mathbf{a}$, $\mathbf{B} = \overline{\mathbf{B}} + \mathbf{b}$ and $\mathbf{J} = \overline{\mathbf{J}} + \mathbf{j}$ respectively, where the overbar represents a local spatial average. We assume a separation of scales such that the lower case quantities vary on scale of inverse wavenumber k_2^{-1} and the overbarred quantities $\overline{\mathbf{B}}$, $\overline{\mathbf{A}}$ vary on scale k_1^{-1} ($0 < k_1 \ll k_2$). We also define a global spatial average taken over the system scale ($\gg k_1^{-1}$), or periodic box. The global averages are indicated by brackets $\langle \rangle$, and being global averages, have no spatial dependence in our approach, only a time dependence.

We define the total average magnetic helicity $H^M = \langle \mathbf{A} \cdot \mathbf{B} \rangle$, and large and small scale averaged magnetic helicities as $H_1^M \equiv \langle \overline{\mathbf{A}} \cdot \overline{\mathbf{B}} \rangle$ and $H_2^M \equiv \langle \mathbf{a} \cdot \mathbf{b} \rangle$, such that $H^M = H_1^M + H_2^M$. The induction equation

$$\partial_t \mathbf{B} = -\nabla \times \mathbf{E} = \nabla \times (\mathbf{v} \times \mathbf{B}) + \lambda \nabla^2 \mathbf{B}, \quad (1)$$

(where \mathbf{v} is the fluctuating velocity, λ is the magnetic diffusivity) and $\mathbf{E} = -\partial_t \mathbf{A} - \nabla \phi$, imply that [6]

$$\partial_t H^M = \partial_t H_1^M + \partial_t H_2^M = -2 \langle \mathbf{E} \cdot \mathbf{B} \rangle = -2 \lambda \langle \mathbf{J} \cdot \mathbf{B} \rangle, \quad (2)$$

where ϕ is the scalar potential. The large and small scale integrated magnetic helicity equations satisfy

$$\partial_t H_1^M = 2 \langle \overline{\mathcal{E}} \cdot \overline{\mathbf{B}} \rangle - 2 \lambda \langle \overline{\mathbf{B}} \cdot \overline{\mathbf{J}} \rangle, \quad (3)$$

and

$$\partial_t H_2^M = -2 \langle \overline{\mathcal{E}} \cdot \overline{\mathbf{B}} \rangle - 2 \lambda \langle \mathbf{b} \cdot \mathbf{j} \rangle, \quad (4)$$

where the turbulent electromotive force $\overline{\mathcal{E}} \equiv \overline{\mathbf{v} \times \mathbf{b}} = -\overline{\mathbf{E}} + \lambda \langle \overline{\mathbf{J}} \cdot \overline{\mathbf{B}} \rangle$. Note that in deriving (4), we have used (2), (3), and the definition of $\overline{\mathcal{E}}$.

For later use, it is helpful to derive relations between globally averaged current helicity, globally averaged magnetic helicity, and globally averaged magnetic energy. For the current helicity we have

$$\langle \mathbf{J} \cdot \mathbf{B} \rangle = -\langle \mathbf{B} \cdot \nabla^2 \mathbf{A} \rangle + \langle \mathbf{B} \cdot \nabla(\nabla \cdot \mathbf{A}) \rangle = -\langle \mathbf{B} \cdot \nabla^2 \mathbf{A} \rangle \quad (5)$$

where the last equality follow from the chain rule, $\nabla \cdot \mathbf{B} = 0$ and the fact that total divergences vanish when globally averaged. Correspondingly, $|\langle \mathbf{b} \cdot \mathbf{j} \rangle| = |k_2^2 H_2^M| \leq k_2 \langle \mathbf{b}^2 \rangle$ and $|\langle \overline{\mathbf{B}} \cdot \overline{\mathbf{J}} \rangle| = |k_1^2 H_1^M| \leq k_1 \langle \overline{\mathbf{B}}^2 \rangle$. The inequalities in the preceding two relations represent the realizability condition [27] and the equality holds for maximally helical (force-free) structures on the respective scales. (These are gauge independent relations because globally averaged divergences vanish. If we had used the Coulomb gauge ($\nabla \cdot \mathbf{A} = 0$), then (5) and the relations above would have followed straight away, without having to appeal to vanishing global divergences.)

The dynamical equation for the turbulent $\overline{\mathcal{E}}$ is

$$\partial_t \overline{\mathcal{E}} = \overline{\partial_t \mathbf{v} \times \mathbf{b}} + \overline{\mathbf{v} \times \partial_t \mathbf{b}}. \quad (6)$$

Therefore, we need equations for $\partial_t \mathbf{b}$ and $\partial_t \mathbf{v}$. Assuming that $\nabla \cdot \mathbf{v} = 0$, subtracting the local mean of (1) from (1) we have

$$\partial_t \mathbf{b} = \nabla \times (\mathbf{v} \times \overline{\mathbf{B}}) + \nabla \times (\mathbf{v} \times \mathbf{b}) - \nabla \times (\overline{\mathbf{v} \times \mathbf{b}}) + \lambda \nabla^2 \mathbf{b}. \quad (7)$$

Similarly, in the absence of any mean velocity, the equation for fluctuating velocity becomes

$$\partial_t \mathbf{v} = \mathbf{v} \times \vec{\omega} - \overline{\mathbf{v} \times \vec{\omega}} - \nabla(p + \mathbf{v}^2/2 - \overline{\mathbf{v}^2}/2) + \mathbf{j} \times \overline{\mathbf{B}} + \overline{\mathbf{J}} \times \mathbf{b} + \nu \nabla^2 \mathbf{v}, \quad (8)$$

where ν is the viscosity and p is the fluctuating pressure. In deriving (8) we assume that $\mathbf{j} \times \mathbf{b} = 0$, from being injected with this property. For simplicity, we also assume that this is maintained at all times (this needs to be tested). This assumption should not affect the basic conclusions from our study because only $\mathbf{j} \cdot \mathbf{b}$ enters the turbulent electromotive force $\overline{\mathcal{E}}$. In addition, we do not assume that the magnetic force associated with the cross-terms between large and small scales are force-free, and thus we still allow terms such as $\mathbf{j} \times \overline{\mathbf{B}}$ and $\overline{\mathbf{J}} \times \mathbf{b}$ to contribute to the small scale magnetic force.

By analogy to Ref. [12], using (7) and (8) we then have for (6)

$$\partial_t \overline{\mathcal{E}} = \frac{1}{3}(\overline{\mathbf{b} \cdot \nabla \times \mathbf{b}} - \overline{\mathbf{v} \cdot \nabla \times \mathbf{v}})\overline{\mathbf{B}} - \frac{1}{3}\overline{\mathbf{v}^2} \nabla \times \overline{\mathbf{B}} + \nu \overline{\nabla^2 \mathbf{v} \times \mathbf{b}} + \lambda \overline{\mathbf{v} \times \nabla^2 \mathbf{b}} + \mathbf{T}, \quad (9)$$

where $T_j = [\overline{\mathbf{v} \times \nabla \times (\mathbf{v} \times \mathbf{b})}]_j - \epsilon_{jqn} \overline{P_{qi}(\mathbf{v} \cdot \nabla v_i) b_n}$ represents the surviving triple correlations (by assuming $\mathbf{j} \times \mathbf{b} = 0$ there no triple correlations survive with more than one factor of \mathbf{b}) and where $P_{qi} \equiv (\delta_{qi} - \nabla^{-2} \nabla_q \nabla_i)$ is the projection operator that arises after taking the divergence of the incompressible Navier-Stokes equation to eliminate the pressure. In deriving (9) we took \mathbf{v} and \mathbf{b} to be statistically isotropic. It will be of interest in future work to drop this assumption [28, 29].

For Eqns. (3) and (4), we want the component of $\overline{\mathcal{E}}$ parallel to $\overline{\mathbf{B}}$. For this we have

$$\partial_t \overline{\mathcal{E}}_{\parallel} = (\overline{\partial_t \mathbf{v} \times \mathbf{b}} + \overline{\mathbf{v} \times \partial_t \mathbf{b}}) \cdot \overline{\mathbf{B}}/|\overline{\mathbf{B}}| + \overline{\mathbf{v} \times \mathbf{b}} \cdot \partial_t (\overline{\mathbf{B}}/|\overline{\mathbf{B}}|). \quad (10)$$

Using Eqns. (9) and (10) we have

$$\partial_t \bar{\mathcal{E}}_{||} = \tilde{\alpha} \bar{\mathbf{B}}^2 / |\bar{\mathbf{B}}| - \tilde{\beta} \bar{\mathbf{B}} \cdot \nabla \times \bar{\mathbf{B}} / |\bar{\mathbf{B}}| - \tilde{\zeta} \bar{\mathcal{E}}_{||} \quad (11)$$

where $\tilde{\alpha} = (1/3)(\overline{\mathbf{b} \cdot \nabla \times \mathbf{b}} - \overline{\mathbf{v} \cdot \nabla \times \mathbf{v}})$, $\tilde{\beta} = (1/3)\overline{\mathbf{v}^2}$, and $\tilde{\zeta} \equiv f k_2 \overline{\mathbf{v}^2}^{1/2}$ accounts for microphysical dissipation terms, the last term of (10), and most importantly, \mathbf{T} . We will take the constant $f \sim 1$, which follows from estimating the magnitude of \mathbf{T} . Note that $\tilde{\zeta}$ and $\tilde{\beta}$ depend on $\overline{\mathbf{v}^2}$ which must be solved for dynamically.

When $\bar{\mathbf{B}}$ is force-free and only one sign of helicity is initially injected into the volume, $\bar{\mathbf{B}} \cdot \bar{\mathbf{J}} \simeq \langle \bar{\mathbf{B}} \cdot \bar{\mathbf{J}} \rangle$ and $\bar{\mathbf{B}}^2 \simeq \langle \bar{\mathbf{B}}^2 \rangle = k_1 |H_1^M|$ [10]. (We consider the injection of one sign to illustrate as simply as possible the tendency for magnetic helicity to inverse cascade. If both signs are injected with equal magnitude then no net magnetic helicity would be injected at all. Also, the source of large scale field growth in the problem we consider comes from the $\bar{\mathcal{E}}$ terms, which grows force-free large scale fields.) In addition, $\overline{\mathbf{v}^2} \simeq \langle \mathbf{v}^2 \rangle$, $\overline{\mathbf{v} \cdot \nabla \times \mathbf{v}} \simeq \langle \mathbf{v} \cdot \nabla \times \mathbf{v} \rangle$, and $\overline{\mathbf{b} \cdot \mathbf{j}} \simeq \langle \mathbf{b} \cdot \mathbf{j} \rangle$. Then (3) and (4) become

$$\partial_t H_1^M = 2\bar{\mathcal{E}}_{||} k_1^{1/2} |H_1^M|^{1/2} - 2\lambda k_1^2 H_1^M \quad (12)$$

and

$$\partial_t H_2^M = -2\bar{\mathcal{E}}_{||} k_1^{1/2} |H_1^M|^{1/2} - 2\lambda k_2^2 H_2^M. \quad (13)$$

Using $U \equiv \langle \mathbf{v}^2 \rangle$, $H_2^V \equiv \langle \mathbf{v} \cdot \nabla \times \mathbf{v} \rangle$, we re-write (11) in the two scale approach as

$$\partial_t \bar{\mathcal{E}}_{||} = k_1^{1/2} |H_1^M|^{1/2} (k_2^2 H_2^M - H_2^V) / 3 - k_1^{3/2} (H_1^M / (|H_1^M|^{1/2}) U / 3 - f k_2 U^{1/2} \bar{\mathcal{E}}_{||}). \quad (14)$$

To solve for the evolution of H_1^M and H_2^M using (14), we also need dynamical equations for U and H_2^V . Our substitution $\overline{\mathbf{v}^2} \simeq \langle \mathbf{v}^2 \rangle$ allows us to ignore boundary terms, since we have stated that $\langle \rangle$ is taken over a closed or periodic volume. Then, from (8),

$$\partial_t U = 2\langle (\mathbf{v} \times \mathbf{j}) \cdot \bar{\mathbf{B}} \rangle - 2\langle (\mathbf{v} \times \mathbf{b}) \cdot \bar{\mathbf{J}} \rangle - 2\nu \langle (\nabla \mathbf{v})^2 \rangle \simeq 2(k_2 - k_1) \langle \bar{\mathcal{E}} \cdot \bar{\mathbf{B}} \rangle - 2\nu k_2^2 \langle \mathbf{v}^2 \rangle, \quad (15)$$

and

$$\partial_t H_2^V = 2\bar{\mathbf{B}} \cdot \langle \vec{\omega} \times \mathbf{b} \rangle (k_2 - k_1) - 2\nu \langle \partial_i v_j \partial_i \omega_j \rangle \simeq 2k_2 (k_2 - k_1) \langle \bar{\mathcal{E}} \cdot \bar{\mathbf{B}} \rangle - 2\nu \langle \partial_i v_j \partial_i \omega_j \rangle, \quad (16)$$

where we consider the case that $H_1^M, H_2^M > 0$, took advantage of $\mathbf{j} \times \mathbf{b} = \bar{\mathbf{J}} \times \bar{\mathbf{B}} = 0$, and again dropped surface terms. We also used $\partial_t \langle \mathbf{v} \cdot \mathbf{b} \rangle = -k_2^2 (\lambda + \nu) \langle \mathbf{v} \cdot \mathbf{b} \rangle$ (showing that $\langle \mathbf{v} \cdot \mathbf{b} \rangle$ decays) to write $\langle \vec{\omega} \times \mathbf{b} \rangle_q = \langle v_s \partial_q b_s \rangle = \langle \mathbf{v} \times \mathbf{j} \rangle_q$ in deriving the penultimate term of (16).

The equations to be solved are thus (12), (13), (14), (15) and (16) after converting them into dimensionless form. We write H_2^M at $t = 0$ as $H_2^M(0)$ and define the dimensionless quantities $h_1 \equiv H_1^M / H_2^M(0)$, $h_2 \equiv H_2^M / H_2^M(0)$, $R_M \equiv \sqrt{H_2^M(0)} / \lambda k_2^{1/2}$, $R_V \equiv \sqrt{H_2^M(0)} / \nu k_2^{1/2}$, $\tau \equiv t k_2^{3/2} \sqrt{H_2^M(0)}$, $Q = -\bar{\mathcal{E}}_{||} / k_2 H_2^M(0)$, $\epsilon = U / k_2 H_2^M(0)$, and $h_v \equiv H_2^V / k_2^2 H_2^M(0)$. Using these in (12), (13), (14), (15) and (16) respectively gives

$$\partial_\tau h_1 = -2Q h_1^{1/2} (k_1 / k_2)^{1/2} - 2h_1 (k_1 / k_2)^2 / R_M, \quad (17)$$

$$\partial_\tau h_2 = 2Qh_1^{1/2}(k_1/k_2)^{1/2} - 2h_2/R_M, \quad (18)$$

$$\partial_\tau Q = -(k_1/k_2)^{1/2} h_1^{1/2} (1/3)(h_2 - h_v) + (k_1/k_2)^{3/2} h_1^{1/2} \epsilon/3 - \epsilon^{1/2} fQ, \quad (19)$$

$$\partial_\tau \epsilon = -2(1 - k_1/k_2)(k_1/k_2)^{1/2} Qh_1^{1/2} - 2\epsilon/R_V, \quad (20)$$

and

$$\partial_\tau h_v = -2(1 - k_1/k_2)(k_1/k_2)^{1/2} Qh_1^{1/2} - 2h_v/R_V \quad (21)$$

(In the simple treatment above we have not coupled in an equation for the non-helical part of the magnetic energy. This would arise for example, from a bulk large scale shear, which we also do not include. A varying fraction of non-helical magnetic energy on the large scale would add a time dependent coefficient ≥ 1 to Q in (17) [30].)

Below we consider two cases C1 and C2: For C1, h_2 takes on an initial value $h_2(0) = 1$, and then evolves according to (18) while for C2, $h_2 = 1$ is fixed for all times. Case C1 corresponds to free relaxation (simulated in Ref. [31]) and case C2 corresponds to driven relaxation. The latter represents injecting h_2 into the system, for example by a potential difference [20, 21] which drives instabilities that keep h_2 steady. In both cases ϵ and h_v satisfy the same equation, so $h_v = \epsilon$ for all times when both are initially small.

III. Discussion of Solutions and Physical Interpretation

Solutions for case C1 with $f = 1$ and different $R_M = R_V$ are shown in Fig. 1. We see that h_1 grows and h_2 depletes in accordance with magnetic helicity conservation, while at the same time $\epsilon = h_v$ grows. This prevents h_1 from equaling $h_2(0) = 1$ due to the backreaction from h_v in (19). Instead, the maximum h_1 occurs at $h_1 \sim h_2 \sim 1/2$, after which resistive terms take over and all quantities decay. If h_v did not grow, then h_1 would reach $h_1 \sim h_2(0) = 1$.

Solutions for case C2 with $f = 1$ are shown in Fig 2. In Fig. 2a and 2b, a significant kinematic regime of duration τ_{kin} in which growth of h_1 is independent of R_M and R_V is evident. The quantity τ_{kin} can be estimated by ignoring the R_M and R_V terms and replacing the time derivatives in (17), (19), (20), and (21) by multiplication by $1/\tau_{kin}$. The end of the kinematic phase occurs when h_v grows large enough to deplete the second term in (19) such that the third term in (19) becomes important. This occurs when $h_v = \epsilon = (1 + k_1/k_2)^{-1}$. Using this, and solving for τ_{kin} from the approximated versions of (17), (19) and (20) gives

$$\tau_{kin} \simeq (3f/2)(k_2/k_1)^2(1 + k_1/k_2)^{1/2}, \quad (22)$$

which is ~ 40 for $k_2/k_1 = 5$ and $f = 1$. Solving for h_1 at t_{kin} , then gives $h_1 \simeq (1 - k_1^2/k_2^2)^{-1} \sim 1$. Thus h_1 grows kinematically up to a value $\sim h_2 = 1$.

After τ_{kin} , R_M and R_V become important. The ratio determines the saturation value of h_1 , while R_V determines the rate of approach to the saturation. That R_V rather than

R_M determines this rate results because the build up of h_v suppresses growth of h_1 and R_V appears in (21) in the diffusion term. We can estimate the final saturation values expected for case C2 by setting the right sides of (17), (19), (20), and (21) equal to zero. The solution is $\epsilon = h_v = (1 + k_1/k_2)^{-1}$, $Q \simeq -(k_1/k_2)^{1/2}(1 - k_1^2/k_2^2)^{-1/2}(R_V R_M)^{-1/2} \ll 1$, and $h_1 = (R_M/R_V)(k_2/k_1)^2(1 - k_1^2/k_2^2)^{-1} \simeq (R_M/R_V)(k_2/k_1)^2$. The saturation value of h_1 can be seen to depend on R_V/R_M in Fig 2c.

For both cases C1 and C2 we have also solved the dynamical equations for $f = 1/10$ (C2 solution plotted in Fig. 2d). This corresponds to a closure in which the damping time in the last term of (19) is ~ 10 . Oscillations appear at early times, similar to what is seen in Ref. [12] for the h_v driven dynamo when $f < 1$ and when the closure is applied to passive transport of a scalar [32, 33]. Unlike the case of Ref. [12] however, h_v evolves here, so the similar sensitivity to f is noteworthy. Here, for $f < 1$, Q oscillates around zero because h_v can grow to be larger than h_1 . The sign of $\partial_\tau Q$ then changes and eventually Q changes sign as well. For $f < 1$, the last term in (19) cannot damp growth of Q fast enough to prevent its sign change. Eventually, the R_V term takes over in (20) and (21), damping the growth of ϵ and the oscillations. The oscillation amplitudes provide a prediction for a given f and a diagnostic for the closure. Note that the rise to the first peak in h_1 corresponds to the end of the kinematic regime. Eqn. (22) shows that τ_{kin} decreases with f , explaining why the first peak occurs earlier for $f < 1$ than the end of the kinematic regime for $f = 1$ (compare Fig. 2d with Fig. 2b).

An important feature of the system of equations (16-20) is that they represent a unified framework for understanding aspects of BOTH kinetic helicity driven helical dynamos and dynamical magnetic relaxation depending on whether the source driving the fluctuations initially supplies kinetic helicity or magnetic helicity. If kinetic helicity is steadily supplied, we have the nonlinear dynamo of Ref. [12]. Then $\partial_t h_2 = \partial_t \epsilon = 0$ and Q is initially dominated by the h_v contribution in (18) which drives growth of the large scale magnetic helicity in (19). The near conservation of magnetic helicity then means that the small scale magnetic helicity h_2 must grow with opposite sign to compensate the growth of h_1 . The growth of h_2 , in turn, offsets the kinetic helicity in the first term on the right of (18), slowing the growth of h_1 in (17), and quenching the system into a steady-state. In contrast, as shown above, when the driving initially supplies h_2 instead of h_v , Q is initially dominated by h_2 . Then h_v grows, offsets h_2 in (18) which in turn quenches the growth of h_1 and again drives the system into a steady-state. In this sense, the kinetic helicity driven dynamo and the magnetically helicity driven dynamos are fully complementary, and their non-linear evolution is explicable by the same set of equations with different initial conditions. In both the kinetic and magnetic helicity driven dynamos, the large scale magnetic helicity incurs an initially fast growth phase (kinematic regime) which is independent of the value of the finite microphysical diffusivities, as long as the driving fluctuation scale is far enough above the diffusive scales.

One important difference between two types of dynamos is that for the kinetic helicity driven dynamo, the large and small scale magnetic helicities have *opposite* signs, whereas for the

magnetically driven dynamo, the large and small scale magnetic helicities have the *same* sign. This is easy to understand and highlights the role of magnetic helicity conservation: In the kinetic helicity driven dynamo, there is initially negligible total magnetic helicity, and the kinetic helicity acts to drive one sign to large scales and the other sign to small scales. In the magnetic helicity driven case, there is a net initial total magnetic helicity injection on small scales and the dynamo acts to drive an inverse transfer of magnetic helicity to large scales.

Coming back to the examples discussed in Sec. I, note that the magnetically dominated dynamo, or dynamical magnetic relaxation is most relevant for astrophysical coronae or laboratory devices, where magnetic helicity is injected into the system and the system evolves to relax dynamically. The kinetic helicity driven dynamo is most relevant inside astrophysical objects, which are not magnetically dominated. Note however that for a star or accretion disk, *both* dynamos can actually operate symbiotically: The kinetic helicity dynamo produces large scale fields inside the disk or star, which then rise to the corona. There the supplied fields are “small scale” with respect to the corona, and can subsequently dynamically relax to larger scales via a magnetically driven dynamo. Rapid generation of the large scale fields in this way can be an important source of large scale coronal magnetic fields for magnetically mediated outflows.

Certainly our simple study herein cannot yet describe the details of astrophysical or laboratory applications in detail, but we have identified some unifying physical principles of magnetically dominated dynamos, kinetic helicity driven dynamos, and dynamical magnetic relaxation which can help guide further work.

IV. Conclusions

We have developed a nonlinear dynamical theory of magnetic relaxation, or equivalently, a magnetically driven large scale helical dynamo. To isolate the basic principles and to facilitate comparison with the simplest numerical simulations, we solved the dynamical magnetic relaxation equations in a closed (or periodic) system. Compared to the h_v driven dynamo of Ref. [12], the role of h_2 and h_v are reversed in dynamical magnetic relaxation: in an h_2 (h_v) driven dynamo, subsequent growth of h_v (h_2) quenches the growth of h_1 . Also, h_1 grows with the same (opposite) sign of h_2 in an h_2 (h_v) driven dynamo. We have found that dynamical magnetic relaxation always involves an initial rapid transfer of magnetic helicity from k_2 to k_1 , independent of R_M and R_V , followed by a slow, R_V dependent evolution of h_1 . When $h_2 = 1$ is fixed, h_1 saturates at $h_1 \simeq (k_2/k_1)^2 R_M/R_V$. When $h_2(0) = 1$ and h_2 is allowed to evolve according to (18), $h_1 \simeq 1/2 \simeq h_2$ at maximum before resistively decaying.

More detailed work is needed to incorporate the principles we have identified to specific laboratory configurations or to magnetized astrophysical coronae of stars and accretion disks. However, our results lead us to predict that significant magnetic relaxation will always occur on dynamical time scales (\sim Alfvén crossing time scales): The large scale magnetic helicity reaches

$\sim 1/2$ the strength of the injection scale helicity during a time τ_{kin} , after which relaxation should be viscously limited. The magnetic Prandtl number and the ratio of large to small scales then determine the ultimate saturation values.

The theory can be fully tested with 3-D MHD numerical experiments in a periodic box in which magnetic helicity is injected at some relatively large wavenumber, say $k_f \sim 5$, with an initially negligible velocity. The overall evolution of the magnetic helicity and kinetic helicity spectra can then be measured as a function of time. Future generalizations must incorporate boundary terms, which can be important in both astrophysical and laboratory contexts.

EB acknowledges DOE grant DE-FG02-00ER54600.

REFERENCES

1. A.P. Kazanstevev, Sov. Phys. JETP, **26** 1031 (1968)
2. S. Kida, S. Yanase, J. & Mizushima, Phys. Fluids **3** 457 (1991)
3. J. Maron, S. Cowley, J. McWilliams, "The Nonlinear Turbulent Dynamo," in press Astrophys. J. (2004)
4. N.E.L. Haugen, A. Brandenburg, W. Dobler, Astrophys. J. Lett., **597**, L141 (2003)
5. A. Pouquet, U. Frisch, J. Léorat, J. Fluid Mech., **77** 321 (1976)
6. H.K. Moffatt, *Magnetic Field Generation in Electrically Conducting Fluids*, (Cambridge University Press, Cambridge, 1978)
7. E.N. Parker, *Cosmical Magnetic Fields*, (Oxford: Clarendon Press, 1979)
8. F. Krause & K.-H. Rädler, *Mean-field Magnetohydrodynamics and Dynamo Theory*, (Pergamon Press, New York, 1980)
9. Ya. B. Zeldovich, A.A. Ruzmaikin, & D.D. Sokoloff, *Magnetic Fields in Astrophysics*, (Gordon and Breach, New York, 1983)
10. A. Brandenburg, Astrophys. J., **550**, 824 (2001)
11. J. Maron & E.G. Blackman, Astrophys. J. Lett. **566**, L41 (2002).
12. E.G. Blackman & G.B. Field, Phys. Rev. Lett., **89**, 265007 (2002)
13. S. Ortolani & D.D. Schnack, *Magnetohydrodynamics of Plasma Relaxation* (World Scientific: Singapore, 1993)
14. H.R. Strauss, Phys. Fluids, **28**, 2786 (1985)
15. H.R. Strauss, Phys. Fluids, **29**, 3008 (1986)

16. A. Bhattacharjee & E. Hameiri, Phys. Rev. Lett. **57**, 206 (1986)
17. J.A. Holmes, B.A. Carreras, P.H. Diamond, & V.E. Lynch, Phys. Fluids, **31**, 1166 (1988)
18. A.V. Gruzinov & P.H. Diamond, Phys. Plasmas, **2**, 1941 (1995)
19. A. Bhattacharjee & Y. Yuan, Astrophys. J., **449**, 739 (1995)
20. P.M. Bellan, *Spheromaks*, (Imperial College Press, London, 2000)
21. H. Ji & S.C. Prager, Magnetohydrodynamics **38**, 191 (2002)
22. J.B. Taylor, Rev. Mod. Phys., **58**, 741 (1986)
23. A.A. Galeev, R. Rosner, G.S. Vaiana, Astrophys. J., **229** 318 (1979)
24. C.J. Schrijver & C. Zwaan, *Solar and Stellar Magnetic Activity*, (Cambridge: Cambridge Univ. Press, 2000)
25. G.B. Field & R.D. Rogers, R.D. Astrophys. J., **403** 94 (1993)
26. E.G. Blackman, MNRAS, **344**, 707 (2003).
27. U. Frisch, A. Pouquet, J. Léorat & A. Mazure, J. Fluid Mech. **68**, 769 (1975).
28. N. Kleeorin & I. Rogachevskii, Phys. Rev. E., **59**, 6724 (1999)
29. I. Rogachevskii & N. Kleeorin, Phys. Rev. E., **64**, 56307 (2001)
30. E.G. Blackman & A. Brandenburg, Astrophys. J. Lett., **584** L99 (2003)
31. T. Stribling, W.H. Matthaeus, & S. Ghosh, J. Geophys. Res., **99**, 2567 (1994)
32. E.G. Blackman & G.B. Field, Phys. Fluids, **15**, L73 (2003)
33. A. Brandenburg, P. Käpylä, A. Mohammed, “Non-Fickian Diffusion and the tau-approximation from numerical turbulence,” astro-ph/0306521, submitted to Phys. Fluids. (2003).

Figure 1: Solutions for $k_1 = 1$, $f = 1$, $k_2 = 5$, (a) $R_M = R_V = 200$, case C1: h_2 free (b) $R_M = R_V = 2000$, case C1: h_2 free The curves in (a) and (b) are identified as follows: h_1 is the thick solid line; h_2 is the thin solid line; h_v is the long dashed line; $-Q$ is the short dashed line.

Figure 2: (a) Same as Fig. 1a, but case C2: fixed $h_2 = 1$. (b) Same as Fig. 1b, but case C2: fixed $h_2 = 1$. (c) h_1 in case C2 for late times: solid curve is for $R_M = 2000$, $R_V = 200$; short dashed curve is for $R_M = R_V = 200$; long dashed curve is for $R_M = R_V = 2000$. (d) Same as (b), but with $f = 1/10$. Notice that $-Q$ now oscillates about 0. The curves in (a) and (b) are identified as follows: At late times (not shown) the oscillations damp, and the solutions are indistinguishable from the $f = 1$ case.

FIGURE 1ab:

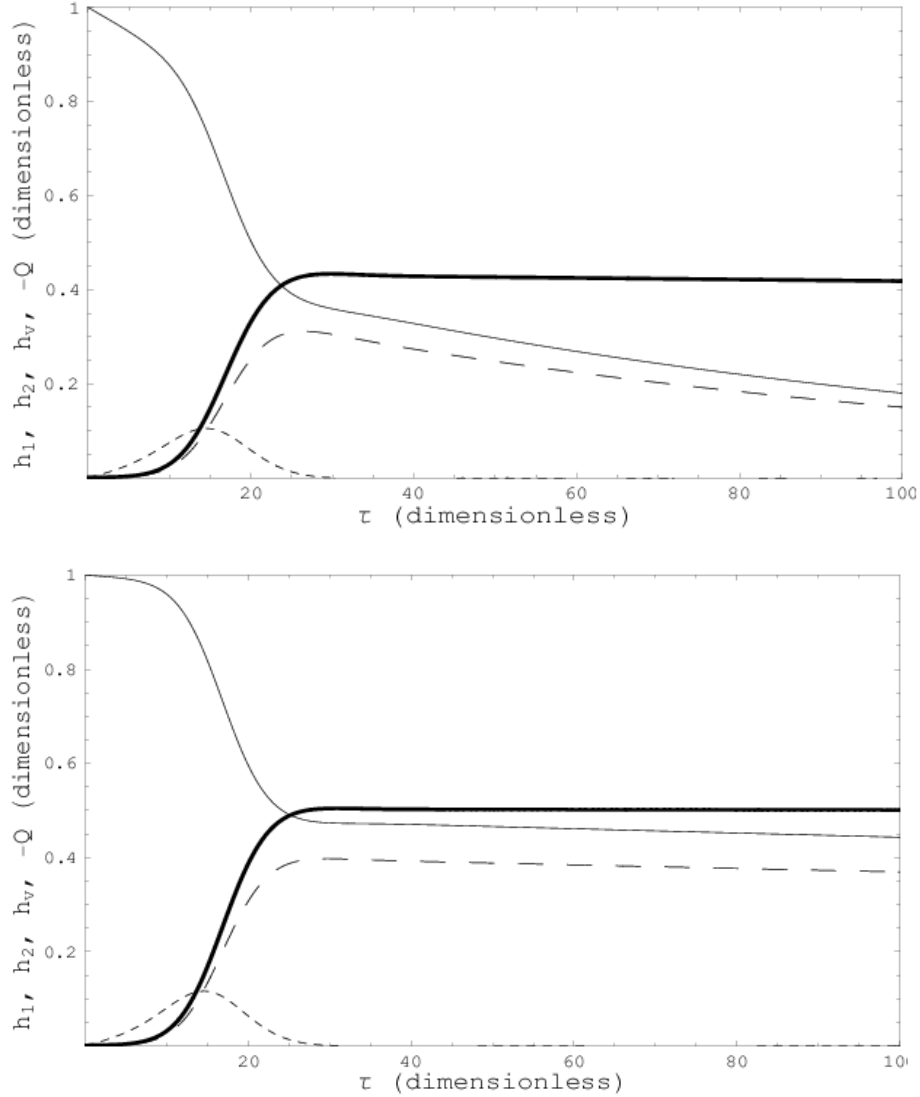


FIGURE 2ab:

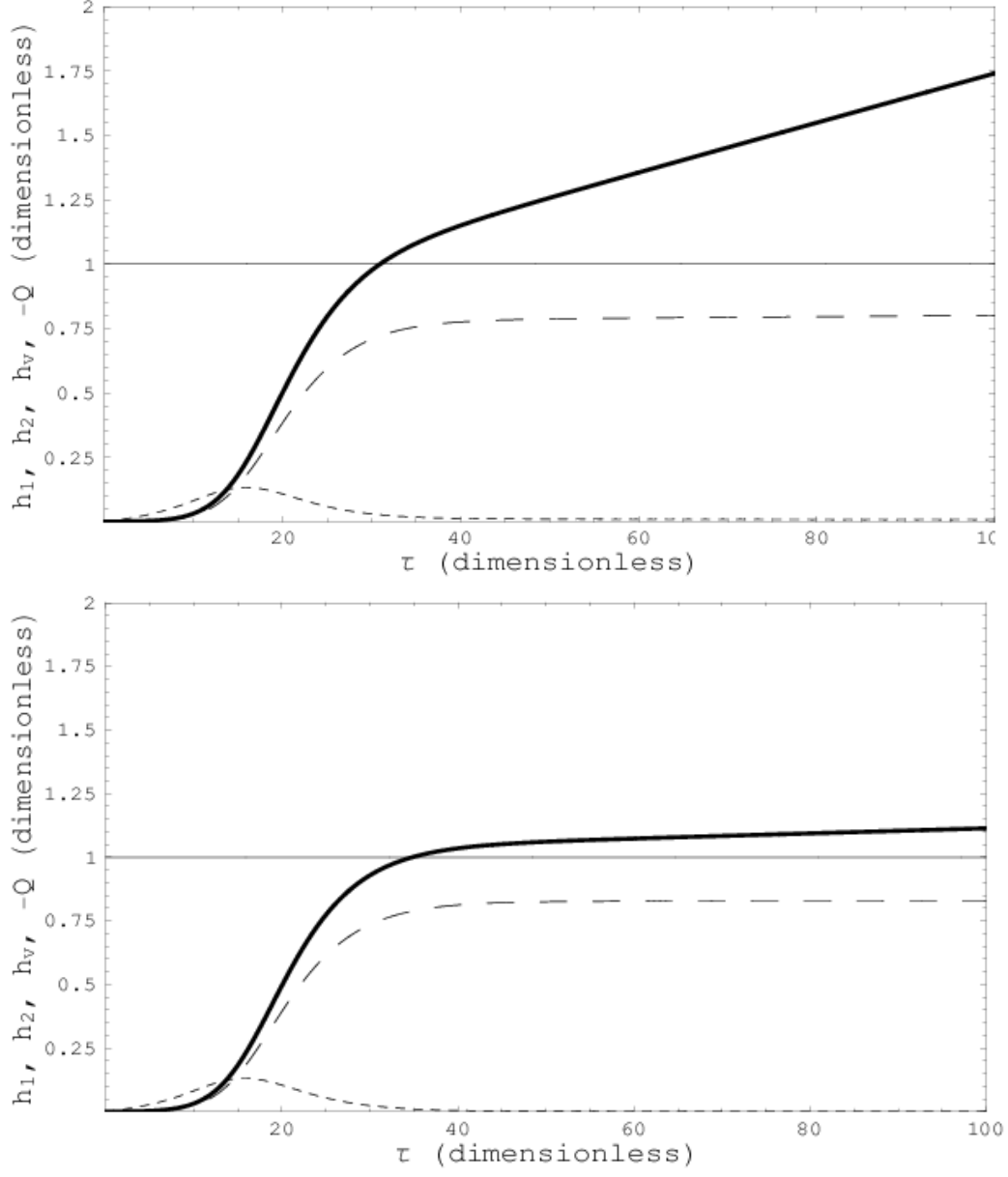


FIGURE 2cd:

